Investigation of Large- and Small-Scale Fading Cross-correlation Using Propagation Graphs

Xuefeng Yin*, Yaoyao Fu*, Jinyi Liang*, and Myung-Don Kim†
*Department of Electronics Science and Technology, Tongji University,
Cao An Road 4800, Dianxin Building, 201804, Shanghai, China,
{yinxuefeng, 1020080066, 1020080067@tongji.edu.cn}
†Electronics and Telecommunications Research Institute, Daejeon, Republic of Korea,
mdkim@etri.re.kr

Abstract

In this contribution, the cross-correlation of the fadings in two propagation channels is studied. It is shown that the behavior of the large-scale fading cross-correlation is determined by the joint spread function (JSF) of the two channels, which describes the correlated behavior of the dispersion of two channels in the parameter space in small-scale. Two parameters are proposed to characterize the JSF which are respectively the maximum of the absolute JSF and the mean of the JSF. Simulations are conducted using a propagation-graph modeling method to investigate the variation of these parameters with respect to the geometry of the environment. The results obtained are valuable for constructing stochastic models for multi-link propagation channels in cooperative relay scenarios.

Keywords: Cross-correlation of channels, channel spread function and joint spread function.

I. Introduction

Cooperative transmission has been adopted in standards of the fourth-generation (4G) wireless communications, such as the Long-Term-Evolution-Advanced (LTE-A) defined in 3GPP documents TR36.814 [1] and TR36.300 [2] and the World Interoperabilty for Microwave Access (WiMAX) systems defined in IEEE802.16. Using cooperative transmission schemes, such as cooperative relays, and cooperative beamforming allows to exploit the uncorrelated multiple channels between the source and multiple transmission nodes for capacity enhancement and interference mitigation. In real cases, a propagation environment can introduce high cross-correlations among the multiple channels, due to *i)* the existence of deterministic components induced by e.g. the line-of-sight (LOS) and the dominant Non-LOS propagation paths and *ii)* similar propagation experienced by the signals in different links. Measurement campaigns in real environments are required to construct realistic stochastic models that can be used to generate multiple correlated channels for system testing and performance evaluation of cooperative transmission techniques. Furthermore, appropriate modeling parameters are necessary which should satisfy the purpose of accurate characterization for correlated channels in cooperative schemes.

The current existing channel models, e.g. the 3GPP spatial channel models (SCM) [3], the WINNER II SCM enhanced models [4], and the IMT-Advanced channel models [5] mainly focus on the channel between a transmitter (Tx) and a receiver (Rx). The joint characteristics, such as the cross-correlation among multiple co-existing channels are neglected. In literature [6], [7], channel models are proposed for large-scale fading cross-correlation in a relay scenario based on measurements. However, the generalization of these models to the scenarios different from that being measured is limited as the models do not show the links between the model parameters and the propagations. In order to establish stochastic models that are applicable for most typical scenarios, it is necessary to establish the models by parameterizing the wideband characteristics of the channels, i.e. the small-scale characteristics of the channel in a multi-dimensional parameter space.

In this contribution, we try to use the joint-characteristics of two channels in the small-scale as an intermediate approach for reproducing the cross-correlation of the channels in large scale. More specifically, the joint-characteristics is represented by the so-called "joint spread function (JSF)" in this paper. In this preliminary study, we propose two parameters to characterize the JSF of two links. In order to understand the behavior of the proposed parameters in realistic environments, channel simulation based on propagation graphs is performed. The impulse responses of co-existing channels are generated and processed to investigate the impact of the different environments on the values of the parameters. The results obtained provide insights when establishing parametric stochastic models for different cooperative schemes based on real measurements.

The rest of the contribution is organized as follows. In Section II, the models of the channel impulse response and the cross-correlation of two channels are presented. Section III describes the parameters proposed for characterizing the joint spread function of two channels. Simulation results obtained based on graph-modeling are introduced in Section IV. Conclusive remarks are provided in Section V.

II. CHANNEL CROSS-CORRELATION COEFFICIENT

Following the nomenclature in [8], the spread function of the channel i in delay τ, Doppler frequency ν, direction of departure $\mathbf{\Omega}_1 \in \mathcal{R}^{3\times 1}$, and direction of arrival $\mathbf{\Omega}_2 \in \mathcal{R}^{3\times 1}$ can be denoted with $h_i(\tau, \nu, \mathbf{\Omega}_1, \mathbf{\Omega}_2)$. For brevity, $h_i(\tau, \nu, \mathbf{\Omega}_1, \mathbf{\Omega}_2)$ is written as $h_i(\boldsymbol{\zeta})$ in the sequel with $\boldsymbol{\zeta} = (\tau, \nu, \mathbf{\Omega}_1, \mathbf{\Omega}_2)$. The channel coefficient α_i at frequency f, time instance t when the Tx and Rx are located at $\boldsymbol{r}_1 \in \mathcal{R}^{3\times 1}$ and $\boldsymbol{r}_2 \in \mathcal{R}^{3\times 1}$ in a rectangular coordinate system respectively is calculated as

$$\alpha_i(t, f, \boldsymbol{r}_1, \boldsymbol{r}_2) = \int_{\mathcal{A}_i} h_i(\boldsymbol{\zeta}) \exp\{j2\pi(f\tau + t\nu + \frac{\boldsymbol{r}_1^{\mathrm{T}}\mathbf{\Omega}_1}{\lambda} + \frac{\boldsymbol{r}_2^{\mathrm{T}}\mathbf{\Omega}_2}{\lambda})\}\mathrm{d}\tau\mathrm{d}\nu\mathrm{d}\mathbf{\Omega}_1\mathrm{d}\mathbf{\Omega}_2 \tag{1}$$

where $\mathcal{A}_i$ denotes the integral region in $\boldsymbol{\zeta}$, λ represents the wavelength of the carrier, and $[\cdot]^{\mathrm{T}}$ is the transpose operation. For the convenience of presentation, notations $\boldsymbol{\eta} = (t, f, \boldsymbol{r}_1/\lambda, \boldsymbol{r}_2/\lambda)$ and the operator $< \boldsymbol{\zeta} \cdot \boldsymbol{\eta} >= (f\tau + t\nu + \frac{\boldsymbol{r}_1^{\mathrm{T}}\mathbf{\Omega}_1}{\lambda} + \frac{\boldsymbol{r}_2^{\mathrm{T}}\mathbf{\Omega}_2}{\lambda})$ are introduced. Thus, (1) is rewritten as

$$\alpha_i(\boldsymbol{\eta}) = \int_{\mathcal{A}_i} h_i(\boldsymbol{\zeta}) \exp\{j2\pi < \boldsymbol{\zeta} \cdot \boldsymbol{\eta} >\}\mathrm{d}\boldsymbol{\zeta}. \tag{2}$$

The cooperative relay scenario is considered where a base station (BS) and a relay station (RS) communicate with a mobile station (MS) simultaneously. The cross-correlation of the channels between the BS and MS, and the channel between the RS and MS is of interest to know for designing such a system. We call the cross-correlation of the channel coefficients α_i and α_j as the LSF cross-correlation of the channels i and j. The "large-scale" is used considering that the channel coefficient is usually calculated via the superposition of the responses of all dispersive components existing in a channel. We first consider the cross-correlation of the coefficients of two channels observed at the same vector $\boldsymbol{\eta}$. Notice that the antenna of the Tx for any of the two channels, is located at $\boldsymbol{r}_1$ with the start of $\boldsymbol{r}_1$ coincident with the center of a small region surrounding the Tx, and similar for the antenna of the Rx in each channel. This LSF cross-correlation coefficient can be calculated as

$$\begin{aligned}\rho_{ij}(\boldsymbol{\eta}) &= \frac{\iint_{\mathcal{A}_i,\mathcal{A}_j} \mathrm{E}[h_i(\boldsymbol{\zeta}_i)h_j^*(\boldsymbol{\zeta}_j)] \exp\{j2\pi < \boldsymbol{\zeta}_i \cdot \boldsymbol{\eta} >\} \exp\{-j2\pi < \boldsymbol{\zeta}_j \cdot \boldsymbol{\eta} >\}\mathrm{d}\boldsymbol{\zeta}_i\mathrm{d}\boldsymbol{\zeta}_j}{\sqrt{\mathrm{E}[\int_{\mathcal{A}} |h_i(\boldsymbol{\zeta})|^2\mathrm{d}\boldsymbol{\zeta}]\mathrm{E}[\int_{\mathcal{A}'} |h_j(\boldsymbol{\zeta})|^2\mathrm{d}\boldsymbol{\zeta}]}} \\ &= \iint_{\mathcal{A}_i,\mathcal{A}_j} p_{ij}(\boldsymbol{\zeta}_i, \boldsymbol{\zeta}_j) \exp\{j2\pi < (\boldsymbol{\zeta}_i - \boldsymbol{\zeta}_j) \cdot \boldsymbol{\eta} >\}\mathrm{d}\boldsymbol{\zeta}_i\mathrm{d}\boldsymbol{\zeta}_j,\end{aligned} \tag{3}$$

where $[\cdot]^*$ represents the complex conjugate,

$$p_{ij}(\boldsymbol{\zeta}_i, \boldsymbol{\zeta}_j) = \frac{\mathrm{E}[h_i(\boldsymbol{\zeta}_i)h_j^*(\boldsymbol{\zeta}_j)]}{\sqrt{P_iP_j}} \quad \text{with} \quad P_{i/j} = \mathrm{E}[\int_{\mathcal{A}_{i/j}} |h_{i/j}(\boldsymbol{\zeta}_{i/j})|^2\mathrm{d}\boldsymbol{\zeta}_{i/j}] \tag{4}$$

is called the joint spread function (JSF) of channels i and j.

III. CHARACTERIZATION

From (3) we see that $\rho_{ij}(\boldsymbol{\eta})$ can be calculated via Fourier transformation of the JSF $p_{ij}(\boldsymbol{\zeta}_i, \boldsymbol{\zeta}_j)$. Thus, it is worthwhile to model the dispersion of $p_{ij}(\boldsymbol{\zeta}_i, \boldsymbol{\zeta}_j)$ in different environments for the cooperative scenarios of interest. The resultant models can be applied to generating co-existing channels in the so-called system level with reasonable $\rho_{ij}(\boldsymbol{\eta})$. Similar to the conventional modeling for single-link channels, the channel JSF $p_{ij}(\boldsymbol{\zeta}_i, \boldsymbol{\zeta}_j)$ can be characterized by using large-scale and small-scale parameters. The large-scale parameters describe the composite property of the general profile of the JSF, and the small-scale parameters characterize individual components in the JSF. In this contribution, we define

$$\check{p}_{ij} = \max(p_{ij}(\boldsymbol{\zeta}_i, \boldsymbol{\zeta}_j); \boldsymbol{\zeta}_i \in \mathcal{A}_i, \boldsymbol{\zeta}_j \in \mathcal{A}_j), \tag{5}$$

$$\bar{p}_{ij} = \frac{1}{\mathcal{A}_i\mathcal{A}_j} \int_{\mathcal{A}_i} \int_{\mathcal{A}_j} p_{ij}(\boldsymbol{\zeta}_i, \boldsymbol{\zeta}_j)\mathrm{d}\boldsymbol{\zeta}_j\mathrm{d}\boldsymbol{\zeta}_i \tag{6}$$

as two large-scale parameters. They represent respectively, the maximum achievable cross-correlation coefficient and the average cross-correlation between arbitrary two points in the channel spread functions $h_i(\boldsymbol{\zeta}_i)$ and $h_j(\boldsymbol{\zeta}_j)$.

As a preliminary study, we use propagation graphs [9] to generate the channel JSF in specific environments and investigate the variability of $\check{p}_{ij}$ and $\bar{p}_{ij}$ with respect to certain geometrical characteristics of the environment.

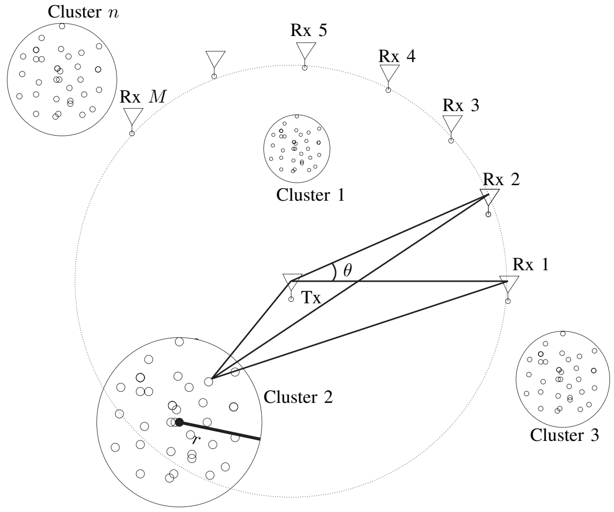

Fig. 1. A propagation graph generated for simulation of the channel impulse responses between a Tx and multiple Rx locations.

IV. Simulation results

In the simulations, propagation graphs are first generated to denote the physical locations of the scatterers, the Tx and Rx. The propagation of electromagnetic waves is modeled as a reverberation process that involves iterative interactions between waves and the scatterers. Monte-Carlo simulations are performed to generate multiple snapshots of channel impulse responses which are used to calculate the JSFs, $\check{p}_{ij}$ and $\bar{p}_{ij}$. In order to investigate the impact of environments on the JSF, the geometrical features of the scatterers, Tx and Rx, are taken as parameters during the simulations.

The propagation environment considered is described in Fig. 1, where the Tx is fixed and the Rx has multiple locations along a circle centered at at the Tx's location. The angle between the line-of-sight (LOS) between Tx and Rx1 and the LOS from Tx to Rx2 is denoted with θ. Scatterers are grouped as clusters. In the simulations, the case where only one group of scatterers are present is considered. The radius of this cluster is denoted with r. The simulations are conducted as follows: for each location of the Rx, totally M snapshots are simulated. In each snapshot, N scatterers are uniformly distributed in a circular region with radius r. For simplicity, we consider only the delay domains. Thus, the channel JSF $p_{ij}(\boldsymbol{\zeta}_i, \boldsymbol{\zeta}_j)$, reduced to $p_{ij}(\tau_i, \tau_j)$ in the considered case, is calculated by taking the average of $h_i(\tau_i)h_j^*(\tau_j)$ obtained in M snapshots, i.e.

$$p_{ij}(\tau_i, \tau_j) = \frac{1}{M} \sum_{m=1} h_i^{[m]}(\tau_i)[h_j^{[m]}(\tau_j)]^* \tag{7}$$

where $h_{i/j}^{[m]}(\tau_{i/j})$ denotes the spread function of the channel i/j observed at mth snapshot. Table I reports the geometrical settings of the environments and the values of the parameters adopted in the simulation. Notice that the cluster radius r and the angle θ between the LOS of the Tx to Rx 1 and the LOS of the Tx to Rx 2 are taken as parameters.

Fig. 2 (a) and (b) depicts respectively the envelope of the variation of $\check{p}_{ij}$ and of $\bar{p}_{ij}$ with respect to r and θ. It is evident from Fig. 2 (a) that the cross-correlation coefficients decrease when r increases. Furthermore, we observed that when θ equals $1.6°$ for the considered case, all cross-correlation coefficients in $p_{ij}(\tau_i, \tau_j)$ are below 0.1 regardless of r. From Fig. 2 (b) we observed that for $\theta < 4.5°$, the average cross-correlation coefficient is positive for all considered r. For $\theta > 4.5°$, $\bar{p}_{ij}$ becomes negative. From Fig. 2 (a) and (b) we also see that it is possible to propose numerical models of $\check{p}_{ij}$ and $\bar{p}_{ij}$ as functions of r and θ. Although the above result is obtained in the single-cluster simulation, it can be generalized to the multiple-cluster scenarios. In the multiple-cluster scenario, each cluster may generate the JSF with $\check{p}_{ij}$ and $\bar{p}_{ij}$ similar to that described by one of the graphs in Fig. 2 (a) and (b). Thus, under the uncorrelated-scattering

TABLE I

Parameter settings in simulations

Item	Value	Item	Value
Height of Rx	10 m	Height of Tx	10 m
Number of Tx locations	1	Number of Rx locations	15
N (Number of scatters)	20	r (Radius of the scatterer cluster)	$0.5, 0.8, 1, 2, 3, 4$ m
Location of Tx (x, y)	$(320, 200)$	Location of the center of scatterers (x, y)	$(345, 150)$
Minimum of θ	$0°$	Maximum of θ	$5.6°$
Step size of θ	$0.37°$	M (Number of snapshots for each Rx location)	2000

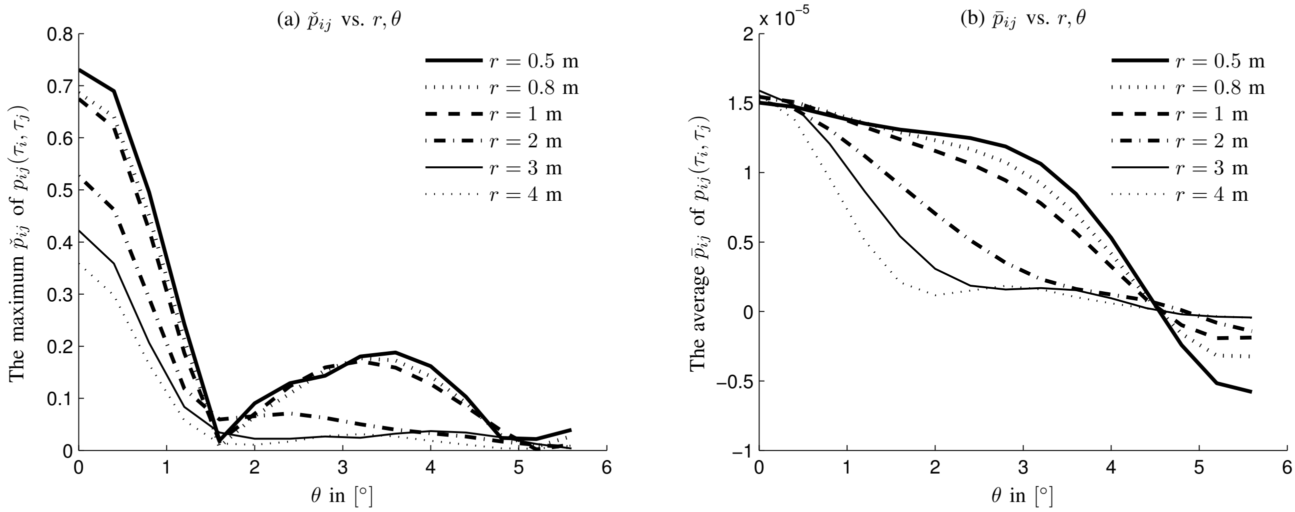

Fig. 2. The $\check{p}_{ij}$ (a) and $\bar{p}_{ij}$ as functions of θ and r.

assumption that the channels generated by different clusters are uncorrelated, $\check{p}_{ij}$ and $\bar{p}_{ij}$ for the channels observed in the multi-cluster scenarios, can be calculated by combining $\check{p}_{ij}$ and $\bar{p}_{ij}$ for the individual clusters.

V. Conclusions

The cross-correlation of the fadings in two channels is closely related to the joint dispersion of the channels in the parameter space, which is described by the "joint spread function (JSF)" proposed here. The maximum and the mean of the JSF have been introduced and used as two large-scale parameters for characterizing the JSF. Models of these parameters based on measurements are of importance for generating correlated multi-link channels. Numerical simulations based on random propagation graphs were performed to study the behavior of the two parameters when the geometrical characteristics of a single-cluster environment varies. Results showed that both the maximum and the mean of the JSF decrease when the cluster radius increases. Fluctuations of the parameters were observed when the angle between the line-of-sight paths in the two channels increases. These results can be generalized to the cases with multiple clusters of scatterers under the uncorrelated scattering assumption.

VI. Acknowledgement

This work was supported by the IT R&D program of KCC/KCA of Korea. [09911-01104, Wideband Wireless Channel Modeling based on IMT-Advanced], the project of the Science and Technology Commission of Shanghai Municipality [10ZR1432700, Multidimensional power spectrum characterization and modeling for wide-band propagation channels], and the China Education Ministry "New-teacher" Project [20090072120015, Time-Variant Channel Characterization, Parameter Estimation and Modeling].

References

[1] *3GPP TR36.814 V9.0.0 (2009) Further Advancements for E-UTRA Physical Layer Aspects (Release 9)*, 3rd Generation Partnership Project; Technical Specification Group Radio Access Network Std., 2009.

[2] *3GPP TS 36.300 v8.7.0 Evolved Universal Terrestrial Radio Access (EUTRA) and Evolved Universal Terrestrial Radio Access Network (EUTRAN); Overall description; Stage 2*, 3rd Generation Partnership Project; Technical Specification Group Radio Access Network Std., Dec. 2008.

[3] "Spatial channel model for Multiple Input Multiple Output (MIMO) simulations (Release 7)," 3GPP TR25.996 V7.0.0, 2007.

[4] "Winner ii channel models," IST-WINNER II Deliverable 1.1.2 v.1.2., IST-WINNER2. Tech. Rep., 2007. [Online]. Available: http://www.ist-winner.corg/deliverables.html996

[5] "Guidelines for evaluation of radio interface technologies for IMT-Advanced," Rep. ITU-R M.2135, 2008.

[6] L. Jiang, L. Thiele, and V. Jungnickel, "Modeling and measurement of MIMO relay channels," in *Proceedings of the Vehicular Technology Conference (VTC Spring)*, May 2008, pp. 419–423.

[7] C.-X. Wang, X. Hong, X. Ge, X. Cheng, G. Zhang, and J. Thompson, "Cooperative MIMO channel models: A survey," *Communications Magazine, IEEE*, vol. 48, no. 2, pp. 80 –87, feb. 2010.

[8] B. H. Fleury, "First- and second-order characterization of direction dispersion and space selectivity in the radio channel," *IEEE Transactions on Information Theory*, no. 6, pp. 2027–2044, Sept. 2000.

[9] T. Pedersen and B. Fleury, "Radio channel modelling using stochastic propagation graphs," in *Communications, 2007. ICC'07. IEEE International Conference on*. IEEE, 2007, pp. 2733–2738.